

## BIAS AND UNCERTAINTY OF PENETRATING PHOTON DOSE MEASURED BY FILM DOSEMETERS IN AN EPIDEMIOLOGICAL STUDY OF US NUCLEAR WORKERS

R. D. Daniels\* and M. K. Schubauer-Berigan

Division of Surveillance, Hazard Evaluations, and Field Studies (DSHEFS), National Institute for Occupational Safety and Health (NIOSH), 555 Ridge Avenue, R-44, Cincinnati, OH 45213, USA

*Received January 5 2005, amended February 1 2005, accepted February 6 2005*

A retrospective exposure assessment of 1269 study subjects was completed for use in a multi-site case-control study of the relationship between protracted workplace external radiation exposure and leukaemia mortality. The majority of exposure data result from film badge monitoring programmes at the four US weapons production facilities and a US Naval shipyard. Bias and uncertainty in reported exposures among study facilities and across time were as result of differences in incident photon energy, exposure geometry, dosimeter type and dosimetry methods. These sources of measurement uncertainty were examined by facility and time to derive bias factors ( $B$ ) for normalising exposures. In conjunction with facility reported results, the bias factors provide a means to estimate the equivalent dose, penetrating to a depth of 10 mm [ $H_p(10)$ ] and the equivalent dose to the active bone marrow for use in the epidemiological study. Uncertainty was expressed as the constructed 95% confidence interval (i.e. the 2.5th–97.5th% range) of the estimated parameter. The bias factors indicate that recorded exposures provide a reasonable estimate of  $H_p(10)$  (bias factor near unity) and overestimate equivalent dose to active bone marrow ( $H_T$ ) by a factor between 1.2 and 1.7. On average, dosimeter-response uncertainties estimated using Monte Carlo simulation were approximately  $\pm 19$  and  $\pm 33\%$  for  $H_p(10)$  and  $H_T$ , respectively.

### INTRODUCTION

The National Institute for Occupational Safety and Health (NIOSH) has conducted a multi-site case-control study to evaluate the relationship between protracted workplace external radiation exposure and leukaemia mortality. Study subjects (1269) consist of radiation workers selected as cases or controls from the Portsmouth Naval Shipyard (PNS) in Kittery, Maine and four major U.S. Department of Energy (DOE) nuclear facilities: Hanford Site, Savannah River Site (SRS), Oak Ridge National Laboratory (ORNL) and the Los Alamos National Laboratory (LANL). A retrospective assessment of protracted exposures to gamma and X-ray irradiation was performed for each study subject. Most of the personal monitoring data used for the assessment originates from worker dosimetry using photographic film emulsions. This paper focuses on the estimation of bias and uncertainty associated with film badge monitoring and the methods used to normalise dosimetry results. The scope is limited to correcting 'detectable' exposures to penetrating photon radiation. For this work, 'penetrating' refers to photons of energies of 100 keV or greater. Although important for epidemiological study, this paper does not address mixed radiation fields, neutron exposures or 'missed' doses resulting from exposures below measurement sensitivity<sup>(1)</sup>.

These sources of uncertainty are being examined further and are anticipated for future publications.

Wide use of film dosimetry began in early 1944 during the development of the A bomb<sup>(2)</sup>. Early Atomic Energy Commission (AEC) facilities (i.e. ORNL, Hanford and LANL) began issuing film badges as primary dosimetry for workers shortly thereafter. In the early 1950s, both PNS and SRS began their dosimetry programmes using film badges. Film badge monitoring continued on a large scale until the emergence of the thermoluminescence dosimeter (TLD) in the mid-1970s.

Many factors have been reported to influence film dosimeter accuracy and sensitivity<sup>(3–6)</sup>. Variations in reported exposures among study facilities and across time resulted from differences in incident photon energy, exposure geometry, dosimeter type, dosimeter calibration and dosimetry methods. Dosimeter response for each facility and monitoring cycle was examined to develop methods for normalising reported doses across study facilities and estimating the dose to the haematopoietic bone marrow for each study subject. Final dose estimates were made by adjusting the exposure records of each facility using dosimeter-specific and facility-specific bias factors.

### METHODS

Site historical records were examined for film dosimeter design, calibration methods, processing equipment and dosimetry procedures. Pertinent data were

\*Corresponding author: RTD2@CDC.gov

gathered, coded into a relational database and indexed by site and time period. Dosimetry histories identified similarities in film emulsion type and design used for penetrating dose interpretation. Dosimeters were grouped, based on these similarities, to simplify the uncertainty analysis.

The uncertainty analysis used the general methods suggested by the National Research Council (NRC)<sup>(7)</sup>. For dose reconstruction of atmospheric test exposures, the NRC combined several sources of dosimetry uncertainty to provide a robust measure of an estimated range of doses that included, with 95% confidence, the true value. For individual dose measurements, the NRC defined a value  $B$  as the bias factor:

$$B = \frac{D_m}{D}, \quad (1)$$

where  $D_m$  is the measured dose and  $D$  is the actual dose value. For  $B > 1$ , the measurement overestimates the true value. Furthermore,  $B$  is distributed log-normally (Equation 2) with geometric mean (GM) and geometric standard deviation ( $S$ ):

$$f(B) = \frac{1}{B\sqrt{2\pi s}} e^{-(\ln(B) - \mu)^2 / 2s^2}, \quad (2)$$

where

$$\text{GM} = e^\mu \quad (3)$$

and

$$S = e^s. \quad (4)$$

Values  $\mu$  and  $s$  are the arithmetic mean and standard deviation of the natural log of  $B$ , respectively. Assuming that bias is actually the product of  $n$  independent factors, each distributed log-normally, then:

$$B_{\text{total}} = \prod_{i=1}^n B_i \quad (5)$$

and  $B_{\text{total}}$  follows a log-normal distribution with a logarithmic standard deviation expressed by:

$$s_{\text{total}} = \sqrt{\sum_{i=1}^n s_i^2}. \quad (6)$$

Finally,  $K$  is a factor such that the interval  $[D_m(KB)^{-1}, D_mKB^{-1}]$  contains  $D$  at the 95% confidence level. For log-normally distributed values,  $K = (S_{\text{total}})^{1.96}$ .

Sources of uncertainty were evaluated in three parts. First, effects related to dosimeter response given varying photon energy and exposure geometry, calibration methods and radiation transport were combined to estimate dosimeter bias and its

associated uncertainty. These sources of error comprise the group of Radiological uncertainties. Second, the uncertainty in exposure results inherent in film processing and dose interpretation was grouped by emulsion type and evaluated as Laboratory uncertainties. Finally, the instability of the film emulsion latent image from varying environmental conditions and film replacement periods results in uncertainty sources grouped as Environmental uncertainties. Overall bias was expressed as the product of individual bias factors needed to normalise reported exposures to estimates of (1) individual equivalent dose at a tissue depth of 10 mm ( $B_{H_p(10)}$ ); and (2) the equivalent dose to the active bone marrow ( $B_{\text{rbm}}$ ).

### Radiological uncertainties

Radiological uncertainties affecting dosimeter response were evaluated for each dosimeter type by combining uncertainties using Monte Carlo simulation. Specific sources of uncertainty evaluated were: (1) exposure geometry, photon energy and organ dose conversion ( $B_{\text{dos}}$ ); (2) calibration methods such as the use of phantoms ( $B_{\text{phantom}}$ ), source field determination ( $B_{\text{cal}}$ ), differing calibration sources ( $B_{\text{Ra}}$ ); and (3) the backscatter ( $B_{\text{bs}}$ ) from the body due to differences in dosimetry placement.

### Dosimeter response ( $B_{\text{dos}}$ )

Values of  $B_{\text{dos}}$  were determined using methods described by Thierry-Chef *et al.*<sup>(8)</sup> Dosimeter energy-geometry-specific bias factors ( $B_{\text{pe,eg}}$ ) were derived for likely ranges of photon energy (pe) and exposure geometry (eg). Photon energies examined included moderate energy photons (100–300 keV) and higher energy photons (300–3000 keV). These spectra were characteristic of most exposures, excluding those associated with radiography, medical and dental X rays, and plutonium processing and finishing. The dosimeter-specific bias factor was estimated from the log-weighted average of the energy-geometry and specific bias factors by:

$$B_{\text{dos}} = \exp \left[ \sum f_{\text{pe}} f_{\text{eg}} \ln(B_{\text{pe,eg}}) \right], \quad (7)$$

where  $f_{\text{pe}}$  is the fraction of exposure from photons within the two energy bands (i.e. 100–300 keV and 300–3000 keV); and  $f_{\text{eg}}$  is the fraction of exposure in the anterior-posterior (AP), rotational (ROT) or isotropic (ISO) exposure geometries.

General exposure conditions were derived for workers from results obtained by Thierry-Chef *et al.*<sup>(9)</sup> and Fix *et al.*<sup>(10)</sup> and from questionnaires completed by study facilities<sup>(11)</sup>. The average values for  $f_{100-300}$  and  $f_{300-3000}$  were 0.2 and 0.8, respectively. For the Monte Carlo simulation,  $f_{100-300}$  was

assumed to be uniformly distributed between 0.15 and 0.25 with  $f_{300-3000}$  set equal to the quantity  $1 - f_{100-300}$ . The value  $f_{AP}$  was assumed uniformly distributed between 0.0 and 1.0. The quantity  $f_{ISO} + f_{ROT}$  was assumed equal to  $1 - f_{AP}$ . Values for  $f_{ISO}$  and  $f_{ROT}$  were solved by the quantities  $f_{ISO} = a(1 - f_{AP})$  and  $f_{ROT} = 1 - f_{ISO}$ , where the variable ( $a$ ) was assumed to follow a triangular distribution between zero and unity, with unity most likely.

Values of  $B_{pe,eg}$  were estimated from response curves developed by Thierry-Chef *et al.*<sup>(8)</sup> and modified to account for the differences in calibration units and to allow reporting equivalent dose to the active bone marrow. Thierry-Chef *et al.* performed a series of experiments using 10 dosimeter types representative of those used at the study facilities over time. These experiments were designed to assess errors associated with dosimetry based on changing exposure conditions<sup>(8)</sup>. Dosimetry response was defined as the ratio of  $H_p(10)$  measured by the dosimeter to  $H_p(10)$  delivered to the dosimeter under controlled conditions<sup>(8)</sup>. Response curves were derived for three photon energies: 118, 208 and 662 keV; and three geometries: AP, ROT and ISO. The response curves related dosimeter response to the energy-absorption coefficient and thickness of the filter used for deep dose determination<sup>(11)</sup>. Each curve follows:

$$b_{pe,eg} = \alpha e^{-\beta X} + \gamma e^{-\delta X}, \quad (8)$$

where  $b_{pe,eg}$  is the dosimeter response or the ratio of  $H_p(10)$  measured to  $H_p(10)$  delivered;  $X$  is the filter density thickness ( $\text{g cm}^{-2}$ ) multiplied by the mass energy-absorption coefficient of the filter material ( $\text{cm}^2 \text{g}^{-1}$ ); and coefficients  $\alpha$ ,  $\beta$ ,  $\gamma$  and  $\delta$  were determined by curve fitting using a non-linear weighted least squares approach (Table 1)<sup>(11)</sup>.

Film badge filter thickness, materials, material densities and mass energy-absorption coefficients (Table 2) were determined for each dosimeter. The material type and thickness were extracted from historical records. Thickness was assumed to be

normally distributed between 95% tolerances of  $\pm 0.05$  mm (0.002 inch). Material densities, except for brass, were extracted from Hubbell and Seltzer<sup>(12)</sup>. Brass density was calculated based on a mixture of 70 wt% copper and 30 wt% zinc using the density values from Hubbell and Seltzer<sup>(12)</sup>. Mass energy-absorption coefficients were determined from curve fitting values for photon energies reported by Hubbell and Seltzer<sup>(12)</sup>.

Since dosimeter response is characterised by the ratio of  $H_p(10)$  measured to  $H_p(10)$  delivered, differences in dose determination methods required adjustments based on the units of the measured result. In earlier years, most facilities actually measured photon exposure in units of Roentgen (R) or milliroentgen (mR), where 1 R is equivalent to  $2.58 \times 10^{-4} \text{ C kg}^{-1}$ . Early reporting of ‘dose’ was often based on the general assumption that 1 R (exposure) equaled 0.01 Sv (equivalent dose). Therefore, reported values were estimates of exposure rather than  $H_p(10)$ . Bias factors were adjusted to estimate equivalent tissue dose ( $H_T$ ) from results ( $\text{C kg}^{-1}$ ) by:

$$B_{pe,eg} = \frac{b_{pe,eg}}{U_{pe} D_{pe,eg}}, \quad (9)$$

where  $b_{pe,eg}$  is the corrected dosimeter response or the ratio of quantity measured to  $H_p(10)$  delivered for a given exposure energy–geometry;  $U_{pe}$  is the ratio of  $H_p(10)$  to unit exposure measured in the appropriate exposure energy–geometry configuration ( $\text{Sv kg C}^{-1}$ ); and  $D_{pe,eg}$  is the ratio of  $H_T$  to  $H_p(10)$  in the appropriate exposure energy–geometry configuration and tissue T is the active bone marrow.

Values for  $U_{pe}$  and  $D_{pe,eg}$  were interpolated for each energy and exposure geometry configuration using combinations of conversion coefficients recommended by the ICRP to convert exposure into kerma free-in-air<sup>(13)</sup>, kerma free-in-air to  $H_p(10)$ <sup>(14)</sup> and kerma free-in-air to  $H_T$ <sup>(14)</sup> (Table 3). To account for uncertainties in interpolating conversion coefficients  $U_{pe}$  and  $D_{pe,eg}$ , the values were assumed to be

**Table 1. Coefficients ( $\alpha$ ,  $\beta$ ,  $\gamma$  and  $\delta$ ) and standard errors (SE) related to the fitted curves for the studied energies and geometries from Thierry-Chef *et al.*<sup>(11)</sup>**

Geometry	Energy	$\alpha$	SE ( $\alpha$ )	$\beta$	SE ( $\beta$ )	$\gamma$	SE ( $\gamma$ )	$\delta$	SE ( $\delta$ )
AP	118	8.33	0.1	1.34	0.02	0	0	0	0
AP	208	1.24	0.06	0.74	0.12	1.16	0.11	47.7	8.89
AP	662	0.9	0.01	—	—	—	—	—	—
ROT	118	6.12	0.11	1.08	0.02	5.92	1.22	63.8	21.3
ROT	208	1.57	0.02	1.37	0.03	2.14	0.45	137.7	25.9
ROT	662	1.06	0.005	—	—	—	—	—	—
ISO	118	4.76	0.26	0.94	0.09	4.31	0.39	34	7.88
ISO	208	1.37	0.02	1.61	0.03	2.54	0.42	149.7	20.7
ISO	662	0.99	0.01	—	—	—	—	—	—

Table 2. Film badge filter characteristics by facility and era used.

ID	Facility	Era	Filter material	Filter thickness (cm)	Filter density $\rho$ (g cm <sup>-3</sup> )	Density thickness (g cm <sup>-2</sup> )	Mass energy-absorption coefficient $\mu_{en} \rho^{-1}$ (cm <sup>2</sup> g)	
							118 keV	208 keV
1	Hanford	1944–1962	Silver	0.10	10.50	1.05	0.68	0.16
	Savannah River Site	1959–1970						
2	Los Alamos National Laboratory	1949–1949	Brass	0.05	8.41	0.43	0.19	0.06
3	Los Alamos National Laboratory	1951–1961	Cadmium	0.05	8.65	0.44	0.71	0.17
4	Portsmouth Naval Shipyard	1952–1974	Cadmium	0.10	8.65	0.87	0.71	0.17
	Savannah River Site	1951–1958						
5	Oak Ridge National Laboratory	1944–1979	Lead	0.05	11.35	0.58	1.65	0.54
	Portsmouth Naval Shipyard	1950–1951						
6	Los Alamos National Laboratory	1944–1948	Lead	0.05	11.35	1.28	0.85	0.27
			Brass	0.08	8.41			
7	Hanford	1962–1972	Tantalum	0.05	16.65	0.85	1.52	0.44

Table 3. Coefficients to convert exposure (C kg<sup>-1</sup>) to equivalent dose, penetrating [ $H_p(10)$ ] and equivalent dose to active bone marrow dose ( $H_T$ ) for selective photon energies and exposure geometries.

Photon energy (keV)	Ratio of $H_T$ to $H_p(10)$ by exposure geometry			Ratio of $H_p(10)$ to exposure for AP geometry (Sv kg C <sup>-1</sup> )
	AP	ISO	ROT	
17	0.024	0.078	0.077	14.1
60	0.303	0.702	0.580	64.1
118	0.478	0.764	0.947	58.3
208	0.528	0.776	0.966	50.2
662	0.631	0.790	0.957	41.0

AP, anterior–posterior; ISO, isotropic; and ROT, rotational

normally distributed about the estimated mean with a standard deviation of 5%. Radiation transport modelling uncertainties introduced when deriving conversion coefficients were not anticipated to exceed 20%<sup>(14)</sup>. Transport modelling uncertainty was assumed normally distributed with a standard deviation of 5%. The coefficient of variation among organ equivalent dose conversion coefficient calculations was <1% for tissues distributed throughout the body<sup>(14)</sup>. As a result, an additional uncertainty of  $\pm 0.5\%$  (95% CI) was assumed for determining dose to the active bone marrow.

$B_{pe,eg}$  was derived from the appropriate  $b_{pe,eg}$  assuming  $b_{300-3000,eg}$  approximately equals  $b_{662,eg}$  and  $b_{100-300,eg}$  is best estimated by the quantity  $xb_{118,eg} + yb_{208,eg}$ , where  $x = 0.25$  and  $y = 0.75$ <sup>(11)</sup>. To account for uncertainties in spectral assumptions,  $y$  was modelled using a beta distribution with

parameters  $\alpha = 15$  and  $\beta = 5$ ; resulting in a negatively skewed distribution with a mean of 0.75 (95% CI = 0.55–0.91). The value  $x$  was set equal to  $1 - y$ .

Attention was given to measurement uncertainty from dosimeter response to competing radiations (e.g. beta or neutron radiation). Although each dosimeter was designed sufficiently to limit response from beta radiation when measuring the deep dose component, a small response may occur from thermal neutron interactions with certain filter materials (e.g. cadmium). Measurement uncertainty resulting from neutron exposures was considered minimal given the low incidence of neutron exposure among study subjects and the use of compensating algorithms during dosimeter processing.

### Calibration uncertainty

Differences in calibration procedures result in uncertainty in dose estimates. For example, free-in-air calibrations do not include the backscatter contribution that would result from dosimeters worn close to the body. Fix *et al.*<sup>(10)</sup> observed that backscatter from the body surface resulted in a 10% contribution to the measured exposure from <sup>137</sup>Cs. Likewise, Delafield<sup>(15)</sup> derived a backscatter factor of 1.09 from <sup>137</sup>Cs irradiation of a 6.35-mm-thick polythene body phantom. Dosimeters calibrated without a phantom were assigned a bias factor ( $B_{phantom}$ ) of  $1.1 \pm 0.05$  (95% CI).

With calibration phantoms, studies have shown that small variations in dosimeter response may result from differences in the backscatter contribution between the various calibration sources and the phantoms used. Brodsky *et al.*<sup>(6)</sup> reported no appreciable backscatter effects from higher energy

gammas emitted by  $^{60}\text{Co}$ , but a 19% increase for  $^{144}\text{Ce}$  (~134 keV). Taylor *et al.*<sup>(16)</sup> reported backscatter contributions of 4 and 8% from phantom calibrations at SRS using  $^{137}\text{Cs}$  and  $^{226}\text{Ra}$ , respectively. Delafield<sup>(15)</sup> reported on-phantom backscatter factors associated with the British ERP-30 film dosimeter of 1.04 and 1.09 using  $^{60}\text{Co}$  and  $^{137}\text{Cs}$ , respectively<sup>(15)</sup>. Based on the literature and normalising to  $^{137}\text{Cs}$  calibration, bias factors ( $B_{\text{phantom}}$ ) of 0.95, 1.0 and 1.05 were assigned for on-phantom calibrations using  $^{226}\text{Ra}$ ,  $^{137}\text{Cs}$  and  $^{60}\text{Co}$  sources, respectively. Calibration geometry, phantom materials, source configuration and dosimeter design play important roles in the dosimeter response from backscatter during calibration, making the assignment of backscatter factors (bias) specific to source isotope uncertain. This uncertainty was assumed to be  $\pm 5\%$ .

Methods used to determine calibration source strength varied from site to site and across time. Some facilities measured the source strength while others used a calculated value. For example, a 4.9% increase in reported doses was observed at SRS beginning in 1987 that was attributed to replacing calculated source strength values with measurements made using a National Bureau of Standards traceable ionisation chamber<sup>(16)</sup>. In some configurations, sources remained stationary during calibration while in others the source was rotated to minimise anisotropy<sup>(17)</sup>. To account for uncertainty in calibration practices across sites, a bias factor ( $B_{\text{cal}}$ ) of  $1.0 \pm 0.05$  was assumed.

It was a common practice to use  $^{226}\text{Ra}$  sources for early film badge calibrations. Given the energy-dependent response of film emulsions, a slight bias may result from calibration using  $^{226}\text{Ra}$  compared with monoenergetic sources. Several experiments regarding the dosimeter energy dependence have been documented<sup>(18-21)</sup>. For a given exposure, the optical density under the filter is independent of photon energies between 0.3 and 2.0 MeV, which is the predominant range for exposures from typical calibration sources. As photon energies decrease, the optical density increases per unit exposure until offset by attenuation of the filter. Peak sensitivities are dependent on the characteristics of the filter and emulsion, but generally occur with photon energies of ~30 keV unfiltered and 100 keV shielded by the deep dose filter. Unlike the monoenergetic photon sources such as  $^{137}\text{Cs}$  and  $^{60}\text{Co}$ , the spectrum from  $^{226}\text{Ra}$  in equilibrium with its progeny is complex and covers a wide range of energies. In addition to higher energy photons from  $^{214}\text{Bi}$  decay, the spectrum includes a low-energy component between 100 and 300 keV<sup>(22)</sup>. Greater optical density per unit exposure may exist for  $^{226}\text{Ra}$  calibrations so that a smaller over-response is observed at low-energy exposures. Facilities where calibrations were performed using  $^{226}\text{Ra}$  were assigned a bias factor ( $B_{\text{Ra}}$ ) of  $1.05 \pm 0.05$ .

### Dosimeter placement

As previously noted, attention was provided to backscatter variability among dosimeter calibrations performed with and without phantoms. On-phantom calibrations were performed to mimic proper placement of the dosimeter on the body surface. However, this is rarely the case in actual monitoring situations because of loose fitting or layered clothing and the use of lanyard and other capture devices. There is uncertainty in backscatter influence given varying dosimeter distances from the body and on-phantom calibrations.

Delafield<sup>(23)</sup> determined backscatter factors for photons exposures in-phantom, on-phantom and at distances from the phantom surface. Delafield's data revealed decreasing backscatter factors with increasing distances from the phantom surface. For example, an on-surface backscatter factor of ~1.1 from  $^{137}\text{Cs}$  exposures was reduced to 1.08 at 2 cm and 1.05 at 5 cm. Likewise, backscatter factors for 206 keV X-ray exposures were ~1.33 on-surface, 1.23 at 2 cm and 1.15 at 5 cm from the phantom surface. A bias factor ( $B_{\text{bs}}$ ) of  $0.95 \pm 0.05$  was assigned to account for dosimeter placement.

### Lower-energy X-ray contribution

Some study subjects were exposed to predominantly low-energy radiation. Plutonium workers at LANL, Hanford, ORNL and SRS were exposed to 17 and 60 keV photons resulting from the decay of  $^{239}\text{Pu}$  and  $^{241}\text{Am}$ . Special calibration and dosimetry techniques were developed by each of the sites to determine low-energy photon exposures. In most cases, a fraction of the low-energy exposure was summed with the results from the more highly penetrating exposures to provide a single effective penetrating radiation result. Although this practice provided for worker protection, deep dose estimates are likely biased high as a result of actual attenuation.

Workers suspected of low-energy photon exposures were identified by review of work histories and dosimetry records. Process records were evaluated for workplace spectra. Dose algorithms used to report results from low-energy photon exposures were examined and efforts were made to separate the more highly penetrating dose component from the contribution of low-energy photon exposures. The uncertainty in dose estimates from low-energy photon exposures was examined using the methods described previously.

### Laboratory uncertainty

Measurement uncertainty results from variation in film processing, determining optical densities and dose interpretation. These errors are assumed to be

not correlated among separate exposure measurements. Even under the most controlled laboratory environments, a relative error of at least 10% was estimated to result from laboratory techniques. This estimate is consistent with values reported by Unruh *et al.*<sup>(24)</sup> following a 2 y study of dosimeter performance capabilities among commercial and government film processors.

Brodsky *et al.*<sup>(6)</sup> demonstrated that film response curves fit the equation

$$\text{NOD} = d_s(1 - e^{-cE}), \quad (10)$$

where NOD is the net optical density above unexposed control films for an exposure  $E$  ( $\text{C kg}^{-1}$ ),  $d_s$  is the saturation density and  $c$  ( $\text{kg C}^{-1}$ ) is the constant for a certain emulsion under fixed exposure and processing conditions. The upper 95% confidence limit for  $E$  was determined by:

$$E_{\text{UCL}} = \frac{\ln \left[ 1 - \frac{\text{NOD} + k\sigma_{\text{od}}}{d_s} \right]}{-c}, \quad (11)$$

where  $k$  is the value for the standard normal deviate that is exceeded with a probability of 0.025 (1.96) and  $\sigma_{\text{od}}$  is the standard deviation of the measured optical density. The value  $K_{\text{lab}}$  was determined for each exposure by dividing the quantity  $E_{\text{UCL}}$  by  $E$ .

Values for  $c$  and  $d_s$  for each film type were interpreted from the calibration curves found in the literature<sup>(6,25-31)</sup>. The value  $\sigma_{\text{od}}$  was estimated over the range of potential exposures by examining replicate density readings recorded during film calibrations at Hanford between 1951 and 1961<sup>(32-34)</sup>.

### Detection level

The scope of the uncertainty analysis was limited to recorded exposures above an estimate of detection. The actual detection level of the film badge is a function of the densitometry and film response. Many factors influenced the minimum dose observed (e.g. densitometry resolution, emulsion type and operator experience). However, theoretical detection levels for each film type can be estimated using methods suggested by Currie<sup>(35)</sup>. A critical level ( $L_C$ ) was determined as the net film density above which the observed response is recognised as 'detected' at 95% confidence. Assuming multiple readings of 'blank' films give net densities that are normally distributed with blank variance  $[\sigma_{\text{od}(B)}]^2$ ,  $L_C \cong 1.645(\sigma_{\text{od}(B)})$ . The detection level ( $L_D$ ) is the net density corresponding to a true signal above which detection is expected at 95% confidence. Therefore,  $L_D = L_C + 1.645(\sigma_{\text{od}(S)})$  where  $\sigma_{\text{od}(S)}$  is the sample net density standard deviation. Assuming  $\sigma_{\text{od}(B)} = \sigma_{\text{od}(S)} = \sigma_{\text{od}}$  at lower film densities,  $L_D$  is approximated by  $3.29\sigma_{\text{od}}$ .

### Environmental uncertainty

Dosimeter calibrations were typically performed under controlled conditions using calibration films exposed in the laboratory and stored in stable environments until processing. In contrast, worker exposures occurred under a wide range of environmental conditions. For example, some film badge readings of shipyard workers at PNS were annotated as 'wet film' or 'dropped in bilge'. There were a number of subjects exposed in laboratories situated in temperate dry climates at LANL. Still others worked in production and maintenance setting in typically hot and humid environments (SRS, ORNL). Several studies on the effects of temperature, humidity and time dependence have been conducted for various film emulsions, some of which are discussed below. Additional historical background on latent image instability can be obtained from Kathren *et al.*<sup>(36)</sup>

Temperature and humidity are expected to vary widely in occupational settings within an industrial facility and across the study sites, resulting in exposure conditions potentially very different from the calibration conditions. These differences result in uncertainty in dose determination when using film dosimeters. Kathren and Brodsky<sup>(5)</sup> reported the average response at 26.5°C and 85% relative humidity which was ~70% ( $0.717 \pm 0.043$ , 1SD) for DuPont Type 555 and 60% ( $0.605 \pm 0.033$ , 1SD) for Kodak Type 2 when compared with the response at zero humidity. This under-response was offset with exposure temperatures approaching 48.9°C. Likewise, Watson<sup>(29)</sup> reported a 40-80% increase in the sensitivity of DuPont Type 502 film exposed at an average temperature of 37°C compared with exposures at room temperature.

A variety of film replacement intervals have been used among and within sites, ranging from weekly (ORNL, Hanford, LANL and SRS) to quarterly (ORNL) monitoring periods. Along with environmental factors, time has been shown to affect latent image stability. Brodsky and Kathren<sup>(3)</sup> reported a loss of precision corresponding to longer film replacement intervals resulting from latent image fading of DuPont Type 555 film. From their experiments, Brodsky and Kathren concluded that doses estimated from bi-weekly monitoring could be low by as much as 30% from latent image fading. Similar tests conducted by Baumgartner<sup>(34)</sup> with DuPont Type 502 film suggests limited latent image fading (~1%) up to intervals of 12 weeks following exposure. In contrast, Baumgartner found that Kodak Type 2 film exhibited a 2-3% increase in image density per month from fogging. Thornton *et al.*<sup>(18)</sup> reported maximum variations in average densities of 5, 15 and 9% for DuPont Types 502, 508 and 555 emulsions, respectively, given exposures over a four month period. Under the same exposure conditions,

the maximum variation of Kodak Type 3 was 15%. Unlike DuPont films, the optical density from the Kodak Type 3 emulsions increased with time since exposure. The contrasting results may be partially explained by the competing nature of image fogging and fading. For example Kathren *et al.*<sup>(36)</sup> observed a linear increase in fogging, similar to the increase reported by Baumgartner<sup>(34)</sup>, that was enhanced by low relative humidity. Kathren *et al.*<sup>(36)</sup> also observed time-dependent latent image fading at relative humidities in excess of 75%. These phenomena are offsetting with a minimal overall effect at ~50% relative humidity.

Sufficient environmental data related to exposures were not available to estimate bias with a high degree of confidence. Others have suggested the uncertainty resulting from environmental conditions can be approximated by assuming a random error of 10% (CI = 95%)<sup>(7,10)</sup>. This approximation seems appropriate given the available literature and the wide range of environmental conditions and monitoring intervals experienced among the study sites.

### Cumulative dose uncertainty

Up to this point, uncertainty estimates pertain to a single badge reading for the 'average worker' of a study facility. However, the summation of dose over several years of exposure (i.e. cumulative dose) is of primary interest in the epidemiological analysis. Measurement uncertainty may change over time as new dosimetry techniques are developed. Likewise, several workers received exposures in multiple study facilities using different dosimetry techniques. The application of different bias factors is straightforward, where the cumulative dose is determined from the sum of bias corrected doses. However, combining uncertainties can be extremely complex and may be impractical without intensive computer simulation. For a simple approximation of combined uncertainties, two general assumptions were made.

First, within a given exposure period, bias and relative uncertainty in dosimeter response characteristics are highly correlated for multiple readings for the same individual. This assumption appears valid given that the worker, work habits, work location and dosimetry are anticipated to remain relatively constant over the exposure period. For perfectly correlated uncertainties, the overall  $K$  from summed results equals  $K$  for a single reading. To account for changing  $K$  among exposure periods, an overall uncertainty was estimated using methods suggested by Fix *et al.*<sup>(10)</sup> where an average of period-specific values for  $K$  was used to approximate overall  $K$ , weighted by the fraction of exposure occurring in the specified period. Exposure periods were defined based on facility assignment and dosimeter type, possessing and calibration.

Second, laboratory uncertainty is not correlated among measurements for the same worker. In this case, the relative uncertainty is inversely proportional to the number of film badge readings used to determine cumulative dose. There is little contribution expected from laboratory uncertainty to the overall uncertainty in the cumulative dose to a worker with a long history of exposure. However, a combined  $K_{\text{lab}}$  value can be approximated by

$$K_{\text{lab}}(\text{combined}) = 1 + \frac{\sqrt{\sum_{i=1}^n [(K_{\text{lab}(i)} - 1)E_i]^2}}{\sum_{i=1}^n E_i}, \quad (12)$$

where  $K_{\text{lab}(i)}$  and  $E_i$  are the lab uncertainty factor and exposure ( $\text{C kg}^{-1}$ ), respectively, for the  $i$ th badge reading of  $n$  monitoring periods.

Although these generalisations provide a means to approximate uncertainty for cumulative doses, it is important to note that a likely bias exists from assuming correlations among worker exposures within an exposure period. Some differences in exposure conditions are likely for a worker, which may reduce the overall relative uncertainty in cumulative doses given offsetting variances.

## RESULTS

### ORNL dosimetry

ORNL began piloting a film meter programme on or about 1 May 1944<sup>(37)</sup>. Film badge data were available for a few study subjects during the time when pocket meters were still the primary dosimetry. Between 1 May 1944 and September 1953, ORNL used a two-element film dosimeter as the primary beta-gamma dosimeter<sup>(37)</sup>. The film dosimeter used a 1 mm cadmium filter with the DuPont Type 552 film packet containing Type 502 sensitive film for low-range penetrating radiation monitoring<sup>(18)</sup>. A four-element dosimeter was introduced in late September 1953, which continued to use cadmium for penetrating radiation<sup>(37)</sup>. The dosimeters used Type 552 or Type 553 film packets, which included Type 502 sensitive film<sup>(38)</sup>. In 1959, the penetrating dose filter was modified to provide for accident-level neutron exposures. The new filter consisted of 0.13 mm gold foil sandwiched between two 0.38 mm cadmium halves<sup>(39)</sup>. During this time, the film packet was changed to the DuPont Type 554, which contained the Type 555 sensitive emulsion. The DuPont Type 554 film packet was later replaced by Eastman Kodak Type 2 between 1968 and 1969. This configuration continued to be used until replaced by TLD technology in 1975.

A film badge calibration jig incorporating 5 cm of plastic to simulate 'backscatter conditions' was first described in late 1953 by Davis *et al.*<sup>(38)</sup> Calibrations were performed using <sup>226</sup>Ra sources<sup>(40)</sup> and were assumed to be performed without a phantom (in-air) before 1954. Documentation of specific dosimeter detection levels could not be located. However, Mitchell *et al.*<sup>(41)</sup> reported the detection level for all ORNL film dosimeters to be  $\sim 7.74 \times 10^{-6} \text{ C kg}^{-1}$ . Dosimetry records demonstrate various recording thresholds. Beginning in 1944, exposures were reported above  $2.58 \times 10^{-6} \text{ C kg}^{-1}$ . By mid-December 1947, the reporting threshold was increased to  $7.74 \times 10^{-6} \text{ C kg}^{-1}$ . The threshold was then reduced to  $2.58 \times 10^{-6} \text{ C kg}^{-1}$  by the mid-1950s.

### SRS dosimetry

The personnel radiation monitoring programme was initiated at SRS in November 1951 using the ORNL two-element film dosimeter<sup>(16)</sup>. Film processing and dose determination were completed at ORNL until March 1953. ORNL dosimetry methods continued to be used until SRS introduced a dosimeter of its own design by November 1959. The SRS dosimeter used DuPont Type 555 sensitive film and a 1 mm silver filter for penetrating radiation determination<sup>(21)</sup>. This design remained essentially unchanged until TLDs became the principal means of beta-gamma measurement on 1 April 1970<sup>(16)</sup>.

Calibrations were conducted at ORNL until March 1952 and then at SRS using <sup>226</sup>Ra. All calibrations were conducted in-air. The reported detection level was  $7.74 \times 10^{-6} \text{ C kg}^{-1}$ .

### Hanford dosimetry

Between October 1944 and March 1957, Hanford used a two-element film dosimeter, consisting of a DuPont Type 552 film packet with Type 502 sensitive film placed between two 1 mm silver filters and a 1 cm<sup>2</sup> window<sup>(42)</sup>. A multi-element film badge replaced the two-element badge in April 1957. The multi-element badge remained in service until replaced by TLDs in January 1972. The multi-element badge also used a 1 mm silver filter for penetrating dose measurement. The multi-element badge briefly used the DuPont 222SX with Type 508 sensitive film<sup>(43)</sup>. By 1960 this film packet was replaced by the DuPont Type 558, which also used Type 508 sensitive film<sup>(43)</sup>. This configuration remained until replaced by TLDs in January 1972<sup>(44)</sup>.

Penetrating radiation calibrations were performed in-air using <sup>226</sup>Ra calibration sources. The dosimeters were calibrated to units of exposure and the approximate detection levels using Type 502 film and Type 508 film were  $1.03 \times 10^{-5}$  and  $5.16 \times 10^{-6} \text{ C kg}^{-1}$ , respectively<sup>(42)</sup>.

### PNS dosimetry

Film badge monitoring began at PNS on 1 July 1950 with Kodak Eastman Type K industrial X-ray film incorporating a 0.5 mm lead filter. In 1952, Eastman DF-7 film replaced the Type K film packet. In 1957, PNS began using a film badge incorporating the DuPont SX-233 film packet with Type 555 sensitive film and a 1 mm cadmium filter. This dosimeter design remained essentially unchanged until July 1969 when the Kodak Type 3 Film Radiac Pack replaced the DuPont film packet. The DT-526/PD calcium fluoride TLD became the standard for personnel gamma exposure monitoring on 1 October 1974<sup>(45)</sup>.

Penetrating radiation calibrations between July 1950 and July 1958 were in-air using <sup>226</sup>Ra calibration sources. Beginning August 1958, calibrations used <sup>60</sup>Co sources and a 10 cm wood block to simulate body mass. In 1964, the shipyard began using <sup>137</sup>Cs for film badge calibrations. Between 1950 and July 1969, the detection threshold was reported to be  $5.16 \times 10^{-6} \text{ C kg}^{-1}$  per monitoring period. With the introduction of Kodak Type 3 film, the detection threshold was reduced to  $2.58 \times 10^{-6} \text{ C kg}^{-1}$ <sup>(45)</sup>.

### LANL dosimetry

Film badges were first distributed to LANL workers in 1944<sup>(46)</sup>. Similar to PNS, the initial badges used Kodak Eastman Type K film packages with a 0.5 mm lead (Pb) cross filter. The film was housed in a sectioned case manufactured from 0.5 mm of brass<sup>(47)</sup>. By late 1947, the lead cross was removed from the Type K film packet and densities from penetrating radiation were determined under the brass filter<sup>(48)</sup>. This basic configuration remained in service until 1949, when a new badge housing was developed consisting of a brass clip which provided for an 'open window' area of the film surface for beta radiation monitoring. This badge used DuPont film Type 552 film packets with DuPont Type 502 sensitive film<sup>(49)</sup>.

Between April and August 1950, LANL issued a new two-filter dosimeter using lead and brass that was designed to provide for energy discrimination<sup>(50)</sup>. Deep dose was determined under the lead filter. This badge was replaced in April 1951 by a similar dosimeter using two 0.5 mm filters, one made of brass and the other made of cadmium<sup>(51)</sup>. The dosimeter used the DuPont 543 film packet with Type 502 sensitive film. Two filters were used in tandem to estimate the effective energy of the gamma or X-ray exposure so that an appropriate energy-response correction factor could be applied to the density under the cadmium filter for the penetrating photon radiation measurement<sup>(20)</sup>. In practice, this correction was applied only in instances



where cadmium densities were comparable to exposures in excess of  $3.87 \times 10^{-5} \text{ C kg}^{-1}$  from photons with an effective energy of 200 keV ( $1.55 \times 10^{-5} \text{ C kg}^{-1}$  of 70 keV;  $5.42 \times 10^{-5} \text{ C kg}^{-1}$  of 25 keV; or  $3.87 \times 10^{-4} \text{ C kg}^{-1}$  of 10 keV)<sup>(52)</sup>. In the summer of 1961, LANL replaced the Type 502 with Type 555<sup>(53)</sup>. This dosimeter configuration remained in widespread use at LANL until fully replaced by the LANL multi-element 'Cyclocac' film badge in 1968<sup>(54)</sup>.

Appearing in October 1962, the Cyclocac film badge was first used by ~100 persons who had histories of appreciable or extraordinary radiation exposures<sup>(55)</sup>. The badge was designed to improve monitoring of low-energy X rays and mixed radiation fields typically encountered with plutonium work. Named after the brand of plastic used in its holder, the Cyclocac badge used two five-element (erbium, tantalum, gold, bismuth and molybdenum or gadolinium) composite filters and an unfiltered area for dose determination<sup>(56)</sup>. The Cyclocac badge was optimised for: (1) gamma and X-ray energy independence (within 30%) from ~30 to 1400 keV; (2) the ability to evaluate thermal neutrons in the presence of X and gamma radiations <400 keV; and (3) improved directional independence. Similar to the brass-cadmium badge, the Cyclocac badge used DuPont Type 502, Type 508 or Type 555 sensitive film depending on availability. By mid-1971, DuPont Type 555 was replaced by Kodak-Eastman Type 2 film<sup>(57)</sup>. Following the discontinuance of the brass-cadmium badge in 1968, the Cyclocac badge remained the primary personal dosimeter at LANL until replaced by TLDs in September 1978<sup>(58)</sup>.

Penetrating radiation calibrations were performed in-air using <sup>226</sup>Ra calibration sources until replaced by <sup>60</sup>Co sources in or about 1960<sup>(51)</sup>. The routine use of calibration phantoms seem to begin on or about 1977<sup>(59)</sup>. The detection threshold for film badge monitoring was reported to be  $1.03 \times 10^{-5} \text{ C kg}^{-1}$  per monitoring period<sup>(58)</sup>.

### Bias and uncertainty factors

Bias and uncertainty factors were estimated for 11 different film dosimeter configurations used at the five facilities (Table 4). The final bias factors demonstrate that facility-reported results were reasonable estimates of  $H_p(10)$  with bias factors ranging from 0.85 to 1.13 and arithmetic mean near unity (0.96; 95% CI = 0.78, 1.16). The average bias factor for active bone marrow dose was 1.39 (95% CI = 1.08, 1.78) with individual bias factors ranging from 1.23 to 1.65, indicating a typical over-response attributable to body attenuation.

Overall, the bias factors were less than earlier estimates by Fix *et al.*<sup>(10)</sup> and by Thierry-Chef *et al.*<sup>(8)</sup>. For example, Fix *et al.* reported an overall

**Table 4. Site-specific bias factors ( $B$ ) and uncertainty factors ( $K$ ) for estimating individual equivalent dose at a tissue depth of 10 mm ( $B_{H_p(10)}$ ,  $K_{H_p(10)}$ ) and equivalent dose to the active bone marrow ( $B_{rbm}$ ,  $K_{rbm}$ ) from recorded exposures.**

$(B_{H_p(10)})$	$(K_{H_p(10)})$	$B_{rbm}$	$K_{rbm}$	Sites and approximate time span
1.02	1.22	1.48	1.28	Hanford (1944–1962); SRS (1951–1969)
0.94	1.23	1.36	1.29	Hanford (1963–1970)
0.96	1.22	1.39	1.29	LANL (1945–1950)
1.13	1.23	1.65	1.31	LANL (1948–1949)
0.91	1.22	1.32	1.28	LANL (1951–1961)
0.87	1.21	1.27	1.28	LANL (1962–1978)
0.98	1.22	1.42	1.29	LANL (1944); PNS (1950–1952)
1.02	1.22	1.49	1.29	PNS (1953–1957); ORNL (1944–1953)
0.89	1.22	1.29	1.28	PNS (1963–1974)
0.93	1.23	1.37	1.30	ORNL (1954–1958)
0.85	1.23	1.23	1.29	ORNL (1959–1974)
0.93	1.22	1.35	1.28	PNS (1958–1963)

bias for 'deep dose' [e.g.  $H_p(10)$ ] and active marrow dose for the Hanford two-element dosimeter of 1.27 (1.13–1.60) and 1.77 (1.43–2.48), respectively. In comparison, this analysis reports bias factors for  $H_p(10)$  and active marrow dose of 1.02 (0.83–1.24) and 1.48 (1.15–1.90), respectively. Much of the differences can be attributed to slightly different energy and geometry assumptions among studies.

The largest over-response ( $B_{H_p(10)} = 1.13$ ) was observed for LANL dosimetry using a single thin brass filter (1947–1950), which provided little attenuation of low-energy X rays. The largest under-response ( $B_{H_p(10)} = 0.85$ ) was observed at ORNL between 1959 and 1974 mostly owing to increased scatter assumed from on-phantom calibration using a radium source.

Table 5 shows the relative contribution to the total variance observed for the most influential variables from the Monte Carlo simulation of the Hanford two-element dosimeter (1944–1956). For  $H_p(10)$  calculations, uncertainty in modelling dose conversion coefficients resulted in the greatest fraction of variability. Both geometry and photon energy had smaller effects on the overall bias or uncertainty for  $H_p(10)$ . However, active bone marrow dose calculations were most influenced by irradiation geometry. Assumptions regarding backscatter, calibration sources and calibration phantoms contributed <10% each to the total uncertainty in  $H_p(10)$  and active bone marrow dose calculations.

The equivalent dose to bone marrow reported for plutonium workers predominantly exposed to low-energy spectra was minimal when compared with more routine exposures. For example, the typical

photon radiation quality encountered by plutonium finishing workers at LANL DP West was characterised by energies of: 17 keV (65–70%), 60 keV (10–20%), 100 keV (1–10%) and >200 keV (0–7%)<sup>(55)</sup>.

**Table 5. Percentage contribution to uncertainty in  $B_{H_p(10)}$  and  $B_{rbm}$  from Monte Carlo analysis of early Hanford two-element film badge<sup>(a)</sup>.**

Variable <sup>(b)</sup>	Percentage contribution to $(B_{H_p(10)})$	Percentage contribution to $B_{rbm}$
$f_{AP}$	5.2	36
$B_{model}$	25	16
$B_{Env}$	25	16
$U_{(662,AP)}$	16	9.7
$B_{bs}$	7	4.4
$B_{cal}$	6.1	3.7
$B_{Ra}$	5.3	3.4
$B_{phantom}$	5.1	3.2
All others	5.3	7.6

<sup>(a)</sup> ( $B_{H_p(10)}$ ) is the final bias factor for individual equivalent dose at a tissue depth of 10 mm.  $B_{rbm}$  is the final bias factor for equivalent dose to the active bone marrow

<sup>(b)</sup>  $f_{AP}$  is the fraction of irradiation in the AP direction.  $B_{model}$  is bias in organ dose conversion from variability in physiology.  $B_{Env}$  is bias from environmental conditions.  $U_{662,AP}$  is the exposure-to-dose conversion for AP irradiation at 662 keV.  $B_{bs}$  is bias from body backscatter.  $B_{cal}$  is bias from calibration methods.  $B_{Ra}$  is bias from radium calibration source.  $B_{phantom}$  is bias from calibration phantom

Using these data in conjunction with appropriate dose conversion coefficients (Table 3) and geometry assumptions, the estimated bias factors for  $H_p(10)$  and active bone marrow dose from plutonium X-ray exposures were 2.9 (1.5–5.6) and 29 (19–44), respectively. Given the low contribution to bone marrow dose, efforts were made to exclude the low-energy component from dose estimates used for the epidemiological study. Where possible, penetrating photon radiation results were extracted from readings only under the shielded portion of the film badge. However, not all workers exposures could be characterised in sufficient detail to exclude the potential for overestimation from reported doses following low-energy exposures.

### Laboratory uncertainty

Values for  $c$  and  $d_s$  for each film type (Table 6) were used to generate and compare film response curves (Figure 1). Slight differences in film sensitivity were observed for the various emulsions used. Overall improvement in sensitivity over time was observed with the introduction of new emulsion types. However, an overall reduction in dosimeter response was observed from the use of filtration.

By using calibration data from dosimeters used during atmospheric nuclear testing, the NRC assumed that  $\sigma_{od}$  was independent of exposure intensity and was  $\sim 0.015$  for DuPont Type 502 film<sup>(7)</sup>. This value is higher than that reported by Baumgartner<sup>(34)</sup>, who conducted experiments with

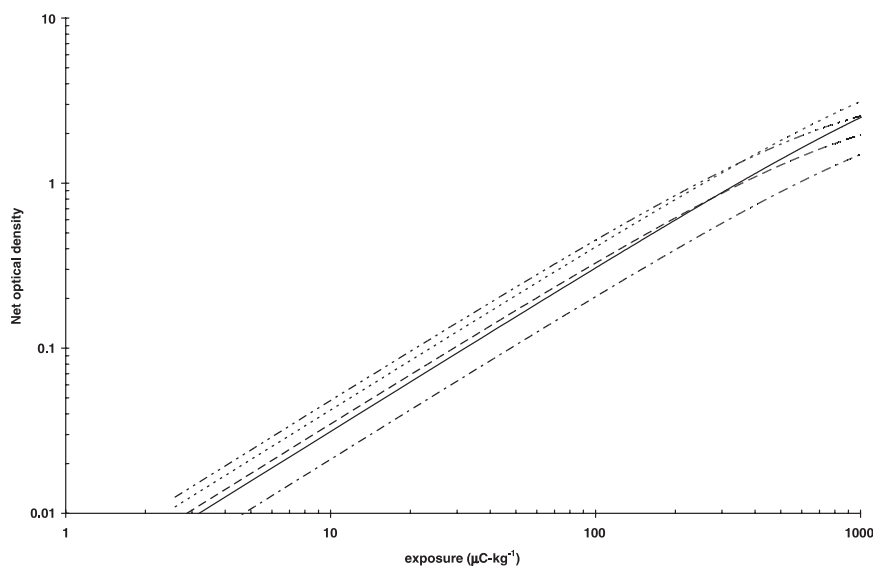


Figure 1. Net optical density vs. exposure for various film emulsions (filtered exposures). DuPont Type 502 (dashed-single dotted line), DuPont Type 508 (dashed line), DuPont Type 555 (continuous line), Eastman Type K (dashed-two dotted line) and Eastman Type 2 (dotted line).

**Table 6. Film saturation densities, sensitivity constants and detection levels.**

Film type	Saturation density $d_s$ (OD)	Sensitivity constant $c$ without filter <sup>(a)</sup> (kg C <sup>-1</sup> )	Sensitivity constant $c$ with filter (kg C <sup>-1</sup> )	Critical level <sup>(b)</sup> $L_C$ ( $\mu\text{C kg}^{-1}$ )	Detection level <sup>(b)</sup> $L_D$ ( $\mu\text{C kg}^{-1}$ )	Filter material	Filter thickness (mm)	Calibration type	Calibration isotope	Reference
DuPont Type 502	2.25	937	755	5.88	11.79	Ag	1	In-air	<sup>226</sup> Ra	(28)
DuPont Type 508	2.69	2490	1300	2.86	5.73	Ag	1	In-air	<sup>226</sup> Ra	(32)
DuPont Type 555	6.60	587	475	3.18	6.37	Ag	1	In-air	<sup>226</sup> Ra	(30)
Eastman Type K <sup>(c)</sup>	3.32	2150	1460	2.06	4.13	(NA)	(NA)	In-air	<sup>226</sup> Ra	(60)
Eastman Type DF-7 <sup>(d)</sup>	3.32	2150	1460	2.06	4.13	(NA)	(NA)	(NA)	(NA)	(NA)
Eastman Type 2	6.60	954	641	2.36	4.72	Pb	0.72	In-air	<sup>60</sup> Co	(31)
Eastman Type 3 <sup>(e)</sup>	6.60	2350	1600	0.94	1.89	(NA)	(NA)	(NA)	(NA)	(NA)

<sup>(a)</sup>Values derived for DuPont films determined without phantom using <sup>60</sup>Co calibration source<sup>(26)</sup>. Eastman-Kodak Type 2 and Type 3 determined free-air using <sup>226</sup>Ra calibration source<sup>(25)</sup>

<sup>(b)</sup>Detection levels calculated for filtered emulsions assuming a minimum optical density standard deviation of 0.006<sup>(33)</sup>.  $2.58 \times 10^{-1} \mu\text{C kg}^{-1} = 1 \text{ mR}$

<sup>(c)</sup>Calibration data were not available for shielded Eastman Type K. A ratio of unshielded to shielded sensitivity of 1.47 was assumed<sup>(60)</sup>

<sup>(d)</sup>Calibration data for Eastman Type DF-7 could not be located. The emulsion is assumed to behave equally to Eastman Type K based on stated similarities<sup>(45)</sup>

<sup>(e)</sup>Calibration data were not available for shielded Eastman Type 3. A ratio of unshielded to shielded sensitivity of 1.47 was assumed<sup>(25,60)</sup>

NA, not available

DuPont Type 502 and Eastman-Kodak Type 2 films that suggested  $\sigma_{\text{od}}$  is proportional to exposure with values between 0.002 and 0.007 for exposures  $< 5.2 \times 10^{-5} \text{ C kg}^{-1}$ . The differences may be attributed, in part, to improvements in densitometry and quality controls between the time of the early nuclear bomb tests and Baumgartner's experiments in 1960. Also, the data used by Baumgartner were carefully controlled to minimise errors in the laboratory-based study. For this study, we evaluated Hanford film calibration data between the years 1951 and 1961 to estimate  $\sigma_{\text{od}}$ . Wilson<sup>(33)</sup> reported the 90% confidence interval (optical density) for replicate density readings from the calibration of DuPont Type 502 film from calibration data between 1951 and 1957. Likewise, Wilson and Larson<sup>(32)</sup> reported similar data for DuPont Type 508 film in support of studies conducted in 1961. Data from Wilson and Larson suggest that  $\sigma_{\text{od}}$  from  $E$  (C kg<sup>-1</sup>) is best approximated by

$$\sigma_{\text{od}} = a + b(1 - e^{-Er}), \quad (13)$$

where the intercept  $a$ , maximum standard deviation  $b$  and rate constant  $r$  are  $6.06 \times 10^{-3}$ ,  $4.32 \times 10^{-2}$

and  $3.23 \times 10^3 \text{ kg C}^{-1}$ , respectively ( $r^2 = 0.78$ ). This approximation was adequate for the range of  $\sigma_{\text{od}}$  determined from the available calibration data (Figure 2).

Values of  $K_{\text{lab}}$  were determined for the various films using Equations 11 and 13. The relative uncertainty associated with film processing is greatest at low exposures. Approximately 100% error ( $K_{\text{lab}} \approx 2$ ) is associated with exposures near detection levels (Figure 3). However, relative uncertainty decreases rapidly with increasing exposure and, for most films, is  $< 30\%$  at  $2.58 \times 10^{-5} \text{ C kg}^{-1}$ .

The values  $L_C$  and  $L_D$  levels were determined for each film assuming  $\sigma_{\text{od}} = 0.006$  (Table 6). The values for  $L_D$  range from 4.72  $\mu\text{C kg}^{-1}$  (18 mR) for Eastman Type 2 film to 11.79  $\mu\text{C kg}^{-1}$  (46 mR) for DuPont Type 502. Calculated  $L_D$  values were compared with the values reported by the study sites and were shown to be in reasonable agreement.

### Cumulative dose

Active bone marrow doses were derived from recorded film badge exposures above the detection threshold and then summed for 10 PNS workers

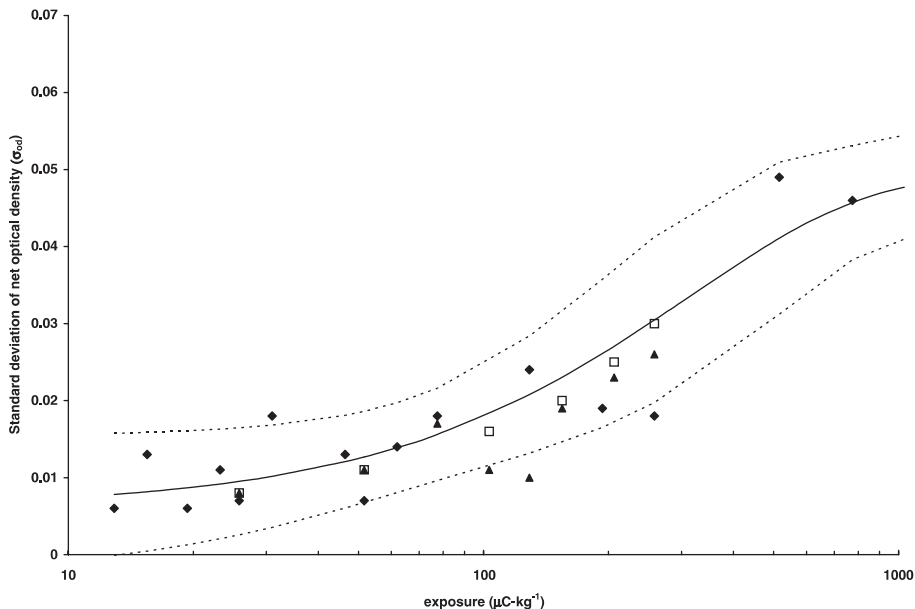


Figure 2. Net optical density standard deviation ( $\sigma_{\sigma_d}$ ) vs. exposure. DuPont Type 508 (filled diamonds), Wilson and Larson<sup>(32)</sup>; DuPont Type 502 (filled triangles), Wilson 1951–1953<sup>(33)</sup>; DuPont Type 502 (open squares), Wilson 1953–1957<sup>(33)</sup>; curve fit of Wilson and Larson data (continuous line); and 95% confidence interval of curve fit (dotted line).

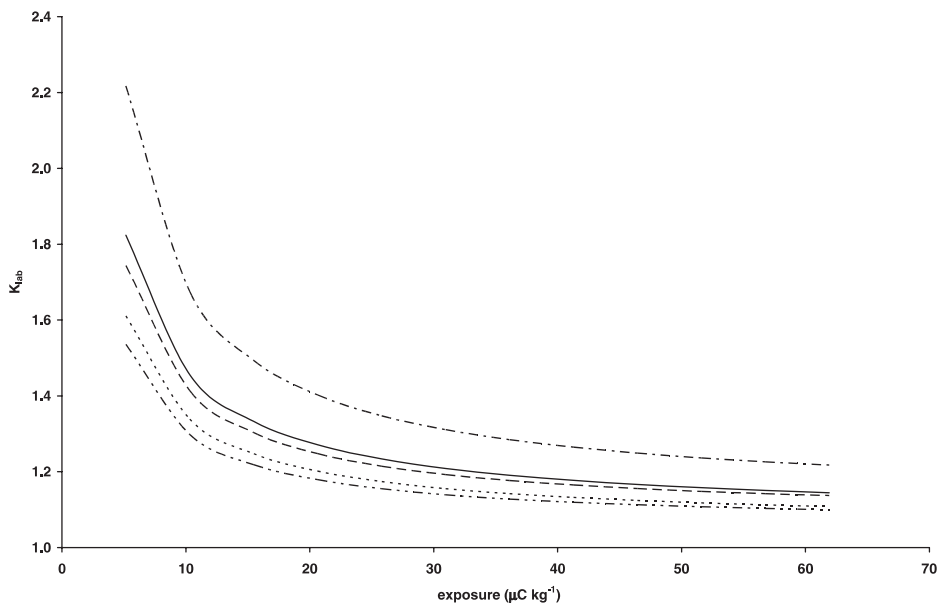


Figure 3. Uncertainty factors ( $K_{lab}$ ) for various film emulsions (filtered exposures). DuPont Type 502 (dashed-single dotted line), DuPont Type 508 (dashed line), DuPont Type 555 (continuous line), Eastman Type K (dashed-two dotted line) and Eastman Type 2 (dotted line).

selected at random. The 95% confidence intervals and final uncertainty factors were determined using Monte Carlo simulation (50 000 trials) and by simple approximation methods (Table 7). Both methods

resulted in comparable confidence intervals. In most cases, the simple approximation method resulted in slightly overestimated uncertainty when compared with the Monte Carlo simulation. However given the

BIAS AND UNCERTAINTY OF PENETRATING PHOTON DOSE

**Table 7. Comparison of confidence intervals (95%) and uncertainty factors (K) for cumulative dose to the active bone marrow from simple approximation and Monte Carlo simulation.**

ID	General statistics		Approximation method CI (95%)			Monte Carlo simulation CI (95%)		
	Number of dose intervals	Cumulative dose (mSv)	Lower	Upper	K	Lower	Upper	K
1	89	39.2	31.3	48.9	1.25	32.1	49.3	1.24
7	46	32.2	25.8	40.2	1.25	26.5	40.5	1.24
9	27	16.5	13.2	20.7	1.25	13.5	20.9	1.25
10	22	40.9	32.7	51.2	1.25	33.6	51.6	1.24
2	4	0.43	0.33	0.56	1.31	0.33	0.57	1.32
3	3	0.2	0.1	0.42	2.1	0	0.46	1.91
6	3	1.54	1.17	2.03	1.32	1.17	2.06	1.33
4	2	0.24	0.13	0.43	1.81	0.06	0.46	1.73
5	2	0.54	0.39	0.74	1.39	0.37	0.76	1.43

complexity of Monte Carlo simulation, the results indicate that a reasonable approximation of uncertainty can be made by simple means.

### CONCLUSIONS

Uncertainties associated with film badge response and processing were evaluated. Bias and uncertainty factors were derived for film dosimetry used by workers at five major radiological facilities between 1944 and 1978. These factors allowed for the estimation of  $H_p(10)$  and the equivalent dose to the active bone marrow for the average worker using the recorded results from a monitoring event. Uncertainty was expressed as the constructed 95% confidence interval (i.e. the 2.5th–97.5th% range) of the estimated parameter.

From derived dosimetric bias factors, recorded exposures appear to provide reasonable estimates of  $H_p(10)$  and overestimates  $H_T$  by a factor between 1.2 and 1.7. On average, dosimeter response uncertainties estimated using Monte Carlo simulation were approximately  $\pm 19$  and  $\pm 33\%$  for  $H_p(10)$  and  $H_T$ , respectively. Unlike estimates of  $H_T$ ,  $H_p(10)$  uncertainty was not significantly influenced by exposure geometry or photon energy under the modelling constraints used.

Laboratory uncertainties were evaluated for the types of emulsion used. Relative uncertainties are greatest near detection levels and may exceed a factor of 2. However, the relative uncertainty is not correlated among individual measurements and may be greatly diminished with doses summed over a long exposure period. A simple approach for applying these factors when summing doses was presented resulting in a method to produce normalised cumulative dose estimates for a multi-site epidemiological study.

### ACKNOWLEDGEMENTS

Funding for this study was provided through an agreement between the DOE and the U.S. Department of Health and Human Services (DHHS). The study was made possible by the cooperation and support of the DOE and U.S. Navy and their employees and contractors. This study particularly benefited from the assistance of the following individuals: Jeff Brann (PNS), Ken Crase (SRS), Russ Morgan (SRS), Elizabeth Dixon (ORNL), Jay McClellan (Hanford), and John Voltin (LANL). In addition, the authors acknowledge the efforts of Jason Flora, Thurman Wenzl, and Dianne Reeder who were instrumental in the records identification, collection, and validation activities.

### REFERENCES

1. Strom, D. J. *Estimating individual and collective doses to groups with 'less than detectable' doses: a method for use in epidemiologic studies.* Health Phys. **51**(4), 437–445 (1986).
2. Pardue, L. A., Goldstein, N. and Wollan, E. O. *Photographic film as a pocket radiation dosimeter.* Report No. CH-1553-A-2223 (Metallurgical Laboratory, Chicago, IL) (1944).
3. Brodsky, A. and Kathren, R. L. *Accuracy and sensitivity of film measurements of gamma radiation. I. Comparison of multiple-film and single-quarterly-film measurements of gamma dose at several environmental conditions.* Health Phys. **9**, 453–461 (1963).
4. Brodsky, A. *Accuracy and sensitivity of film measurements of gamma radiation. II. Limits of sensitivity and precision.* Health Phys. **9**, 463–471 (1963).
5. Kathren, R. L. and Brodsky, A. *Accuracy and sensitivity of film measurements of gamma radiation. III. Effects of humidity and temperature during gamma irradiation.* Health Phys. **122**, 769–777 (1963).
6. Brodsky, A., Spritzer, A. A., Feagin, F. E., Bradley, F. J., Karches, G. J. and Mandelberg, H. I.

- Accuracy and sensitivity of film measurements of gamma radiation. IV. Intrinsic and extrinsic errors.* Health Phys. **11**(10), 1071–1082 (1965).
7. National Research Council. *Film badge dosimetry in atmospheric nuclear tests.* (Washington, DC: National Academy Press) (1989).
  8. Thierry-Chef, I., Pernicka, F., Marshall, M., Cardis, E. and Andreo, P. *Study of a selection of 10 historical types of dosimeter: variation of the response to  $H_p(10)$  with photon energy and geometry of exposure.* Radiat. Prot. Dosim. **102**(2), 101–113 (2002).
  9. Thierry-Chef, I., Cardis, E., Ciampi, A., Delacroix, D., Marshall, M., Amoros, E. and Bermann, F. *A method to assess predominant energies of exposure in a nuclear research centre—Saclay (France).* Radiat. Prot. Dosim. **94**(3), 215–225 (2001).
  10. Fix, J. J., Gilbert, E. S. and Baumgartner, W. V. *An assessment of bias and uncertainty in recorded dose from external sources of radiation for workers at the Hanford site.* PNL-10066 (Pacific Northwest Laboratory, Richland, WA) (1994).
  11. Thierry-Chef, I. *et al.* *International collaborative study of cancer risk among radiation workers in the nuclear industry, study of errors in dosimetry* (International agency on Cancer Research, Lyon, France) (in publication).
  12. Hubbell, J. H. and Seltzer, S. M. *Tables of X-ray mass attenuation coefficients and mass energy-absorption coefficients (version 1.03).* Available on <http://physics.nist.gov/xaamdi> (2003).
  13. International Commission on Radiological Protection. *Data for use in protection against external radiation.* ICRP Publication 51. Ann. ICRP **17**(2–3) (Oxford: Pergamon Press) pp. 1–132 (1988).
  14. International Commission on Radiological Protection. *Conversion coefficients for use in radiological protection against external radiation. Adopted by the ICRP and ICRU in September 1995.* ICRP Publication 74. Ann. ICRP **26**(3–4) (Oxford: Pergamon Press) pp. 1–205 (1996).
  15. Delafield, H. J. *Gamma-ray exposure measurements in a man phantom related to personnel film dosimetry.* Phys. Med. Biol. **11**(1), 63–73 (1966).
  16. Taylor, G. A., Crase, K. W., LaBone, T. R. and Wilkie, W. H. *A history of personnel radiation dosimetry at the Savannah River Site.* Report No. WSRC-RP-95-234 (Westinghouse Savannah River Co., Aiken, SC) (1995).
  17. Wilson, R. H., Milligan, V. M., Unruh, C. M. and Larson, H. V. *Gamma calibration and evaluation techniques for Hanford beta-gamma film badge dosimeters.* Report No. HW-71702 (Hanford Laboratories Operation, General Electric Co., Richland, WA) (1960).
  18. Thornton, W. T., Davis, D. M. and Gupton, E. D. *The ORNL badge and its personnel monitoring applications.* Report No. ORNL-3126 (Oak Ridge National Laboratory, Oak Ridge, TN) (1961).
  19. Kocher, L. F., Bramson, P. E. and Unruh, C. M. *The new Hanford film badge dosimeter.* Report No. HW-76944 (Hanford Laboratories, Richland, WA) (1963).
  20. Storm, E. *The response of film to X-radiation of energy up to 10 MeV.* Report No. LA-1220 (Los Alamos National Laboratory, Los Alamos, NM) (1951).
  21. Wright, C. N. *Data on new film badge.* Letter to File (Savannah River Site, Aiken SC) 1 December (1959).
  22. Kathren, R. L. and Church, L. B. *Mean and effective photon energies of  $^{226}\text{Ra}$  in equilibrium with daughters.* Health Phys. **30**(1), 143–145 (1976).
  23. Delafield, H. J. *Gamma ray exposure measurements in a man phantom related to personnel film dosimetry.* Report No. AERE-4430 (Health Physics and Medical Division, Atomic Energy Research Establishment, Harwell, Berkshire, UK) (1963).
  24. Unruh, C. M., Larson, H. V. and Beetle, T. M. *Film dosimeter performance criteria and assessment of current performance levels.* Report No. BNWL-SA-1836 (Battelle Memorial Institute, Pacific Northwest Laboratory, Richland, WA) (1968).
  25. KODAK. *Kodak personal monitoring films,* Seventh edn. KODAK Pamphlet No. P-31 (Eastman Kodak Co., Rochester, NY) (1968).
  26. Du Pont. *Dosimeter Film* (E. I. Du Pont De Nemours & Co., Inc., Wilmington, DEL) (1956).
  27. Keck, A. H. *Dose-density characteristics of Du Pont type 555 film packets—(with lead backing).* Report No. HW-45504 (Hanford Works, Richland, WA) (1956).
  28. Larson, H. V. and Roesch, W. C. *Gamma dose measurement with Hanford film badges.* Report No. HW-3256 (Hanford Works, Richland, WA) (1954).
  29. Watson, E. C. *Preliminary investigation of DuPont film types.* Report No. HW-23862 (Hanford Works, Richland, WA) (1952).
  30. Nelson, I. C. *Dose-density characteristics of Dupont SX-233 film.* Report No. HW-39179 (Hanford Atomic Products, Richland, WA) (1955).
  31. REECO. *Photographic dosimetry.* Report No. RRS-57-1 (Reynolds Electrical & Engineering Co., Inc.) (1957).
  32. Wilson, R. H. and Larson, H. V. *Film calibration for high level dose evaluation.* Report No. HW-71133 (Hanford Works, Richland, WA) (1961).
  33. Wilson, R. H. *Reproducibility of personnel monitoring film densities.* Report No. HW-51934 (Hanford Works, Richland, WA) (1957).
  34. Baumgartner, W. V. *Some studies of film dosimeter variables.* Report No. HW-SA-2032 (Hanford Works, Richland, WA) (1960).
  35. Currie, L. A. *Limits for qualitative detection and quantitative determination: application to radiochemistry.* Anal. Chem. **40**, 586–593 (1968).
  36. Kathren, R. L., Zurakowski, P. R. and Covell, M. *Effect of humidity and dose on latent image stability.* Am. Ind. Hyg. Assoc. J. **27**(4), 388–395 (1966).
  37. Hart, J. C. *A progress report dealing with the derivation of dose data from ORNL personnel exposure records applicable to the Mancuso study.* Report No. 66-1-84 (Oak Ridge National Laboratory, Oak Ridge, TN) (1966).
  38. Davis, D. M., Gupton, E. D. and Hart, J. C. *Applied health physics radiation survey instrumentation,* First edn. Report No. ORNL-332 (Oak Ridge National Laboratory, Oak Ridge, TN) (1954).
  39. Hurst, G. S. and Ritchie, R. H. *Radiation accidents: dosimetric aspects of neutron and gamma-ray exposure,* Second edn. Report No. ORNL-2748 (Oak Ridge National Laboratory, Oak Ridge, TN) (1961).

BIAS AND UNCERTAINTY OF PENETRATING PHOTON DOSE

40. Craft, H. R., Ledbetter, J. C. and Hart, J. C. Health Physics Division. *Personnel monitoring operating techniques*. Report No. ORNL 1411 (Oak Ridge National Laboratory, Oak Ridge, TN) (1953).
41. Mitchell, T. J., Ostrouchov, G., Frome, E. L. and Kerr, G. D. *A method for estimating occupational radiation dose to individuals, using weekly dosimetry data*. Report No. ORNL-6778 (Oak Ridge National Laboratory, Oak Ridge, TN) (1993).
42. Wilson, R. H., Fix, J. J., Baumgartner, W. V. and Nichols, L. L. *Description and evaluation of the Hanford personnel dosimeter program from 1944 through 1989*. Report No. PNL-7447 (Pacific Northwest Laboratory, Richland, WA) (1990).
43. Wilson, R. H. *Historical review of personnel dosimetry development and its use in radiation protection programs at Hanford*. Report No. PNL-6125 (Pacific Northwest Laboratory, Richland, WA) (1987).
44. Nichols, L. L., Endres, G. W. R., Shipler, D. B., Oscarson, E. E. and Crass, L. L. *Hanford multipurpose TL dosimeter field tests and evaluation*. Report No. BNWL-B-127 (Battelle Pacific Northwest Laboratories, Richland, WA) (1972).
45. Portsmouth Naval Shipyard. *A historical report on the standards and instrumentation for radiological controls*. Report No. RC-105-1 (Portsmouth Naval Shipyard, Portsmouth, New Hampshire) (1980).
46. Hempleman, L. H. Letter to S. L. Warren (Los Alamos National Laboratory, Los Alamos, NM) 18 May (1944).
47. Ferry, J. L. *Transmittal of report: use of lead cross Type K dental film packets to monitor gamma ray, x-ray, and beta-ray exposures*. Letter to H. T. Wensel (Manhattan Engineering District, Oak Ridge, TN) 27 October (1944).
48. Buckland, C. *Los Alamos health group film badge procedures*. Report No. LAMS-620 (Los Alamos National Laboratory, Los Alamos, NM) (1947).
49. Littlejohn, G. *Method of reporting beta exposure on personnel exposure reports*. Letter to File (Los Alamos National Laboratory, Los Alamos, NM) 10 January (1949).
50. Lawrence, J. P. *Film badge techniques*. Letter to File (Los Alamos, National Laboratory, Los Alamos, NM) 4 October (1956).
51. Littlejohn, G. J. *Photodosimetry procedures at Los Alamos*, 16th edn. Report No. LANL LA-2494 (Los Alamos, National Laboratory, Los Alamos, NM) (1961).
52. Lawrence, J. N. P. *Re: Beta calibration*. Letter to F. L. Paschal Jr (Los Alamos National Laboratory, Los Alamos, NM) 4 October (1956).
53. Littlejohn, G. J. *Photodosimetry procedure books: changes in evaluation procedures*. Letter to File (Los Alamos National Laboratory, Los Alamos, NM) 20 March (1963).
54. LASL. *The new LASL film badge and personnel neutron dosimetry packet*. Report No. LA-3889 (Los Alamos National Laboratory, Los Alamos, NM) (1968).
55. Dummer, J. E. *Correlation between brass-cadmium and cyclocac film badges*. Letter to D. D. Meyer (Los Alamos National Laboratory, Los Alamos, NM) 5 March (1963).
56. Storm, E. S. S. *Nuclear radiation dosimeter using composite filter and a single element filter*. United States 3130306, United States Atomic Energy Commission, 21 April (1964).
57. Lawrence, J. P. *Eastman Type II open window factors*. Letter to File (Los Alamos National Laboratory, Los Alamos, NM) 1 May (1973).
58. Lawrence, J. P. *Reportable TLD exposures*. Letter to File (Los Alamos National Laboratory, Los Alamos, NM) 28 September (1978).
59. Storm, E., Cortex, J. R. and Littlejohn, G. J. *Calibration of personnel dosimeters*. Report No. LA-UR-77-2613 (Los Alamos National Laboratory, Los Alamos, NM) (1977).
60. Wright, C. N. *Test of Eastman Type 1 personal monitoring film*. Letter to W. L. Marter (Savannah River Plant, Aiken, SC) 17 July (1958).